

# Possible role of flexible red blood cell membrane nanodomains in the growth and stability of membrane nanotubes

Aleš Iglič<sup>a,\*</sup>, Maruša Lokar<sup>a</sup>, Blaž Babnik<sup>a</sup>, Tomaž Slivnik<sup>a</sup>, Peter Veranič<sup>b</sup>,  
Henry Hägerstrand<sup>c</sup>, Veronika Kralj-Iglič<sup>d</sup>

<sup>a</sup> *Laboratory of Physics, Faculty of Electrical Engineering, University of Ljubljana, Ljubljana, Slovenia*

<sup>b</sup> *Institute of Cell Biology, Faculty of Medicine, University of Ljubljana, Ljubljana, Slovenia*

<sup>c</sup> *Department of Biology, Åbo Akademi University, Biocity, Åbo/Turku, Finland*

<sup>d</sup> *Laboratory of Clinical Biophysics, Faculty of Medicine, University of Ljubljana, Ljubljana, Slovenia*

Submitted 3 February 2007

Available online 1 May 2007

(Communicated by J.F. Hoffman, Ph.D., 6 March 2007)

## Abstract

Tubular budding of the erythrocyte membrane may be induced by exogenously added substances. It is shown that tubular budding may be explained by self-assembly of anisotropic membrane nanodomains into larger domains forming nanotubular membrane protrusions. In contrast to some previously reported theories, no direct external mechanical force is needed to explain the observed tubular budding of the bilayer membrane.

The mechanism that explains tubular budding may also be responsible for stabilization of the thin tubes that connect cells or cell organelles and which might be important for the transport of matter and information in cellular systems. It is shown that small carrier vesicles (gondolas), transporting enclosed material or the molecules composing their membrane, may travel over long distances along the nanotubes connecting two cells.

© 2007 Elsevier Inc. All rights reserved.

*Keywords:* Membrane nanodomains; Tubular budding; Self-assembly; Transport through nanotubes; Membrane nanovesicles

## Introduction

Exogenously added amphiphilic substances (detergents, peptides) bind readily into the red blood cell membrane, thereby causing cell shape changes. According to the bilayer couple hypothesis, the transformation of echinocyte shape is driven by binding of the exogenously added molecules preferentially into the outer membrane layer (Fig. 1). When red blood cells approach to the type III echinocytic shape, budding and nanoexovesicle release (spherical or tubular) from the membrane surface starts (Fig. 1).

It has been shown that the stability of the echinocyte shape is primarily determined by competition between the membrane bilayer Helfrich–Evans bending energy and the membrane

skeleton shear energy [2]. A constitutive model for membrane skeleton behaviour takes into account that the membrane skeleton is locally compressible [3–5]. However, for reasons of simplicity the membrane skeleton shear energy is usually calculated using an approximate expression [6,2]:

$$W_{\text{shear}} = \frac{\mu}{2} \int (\lambda_m^2 + \lambda_m^{-2} - 2) dA, \quad (1)$$

where the membrane skeleton is considered laterally incompressible [7],  $\mu$  is the membrane skeleton area shear modulus,  $\lambda_m$  is the principal extension ratio along the meridional direction [6,2] and  $dA$  is the membrane area element. The Helfrich–Evans membrane bending energy is the sum of a local and a non-local term [6,8–10]:

$$W_b = \frac{k_c}{2} \int (2H)^2 dA + k_n A (\langle H \rangle - H_0)^2 \quad (2)$$

\* Corresponding author. Fax: +386 1 4768 850.

E-mail address: [ales.iglic@fe.uni-lj.si](mailto:ales.iglic@fe.uni-lj.si) (A. Iglič).

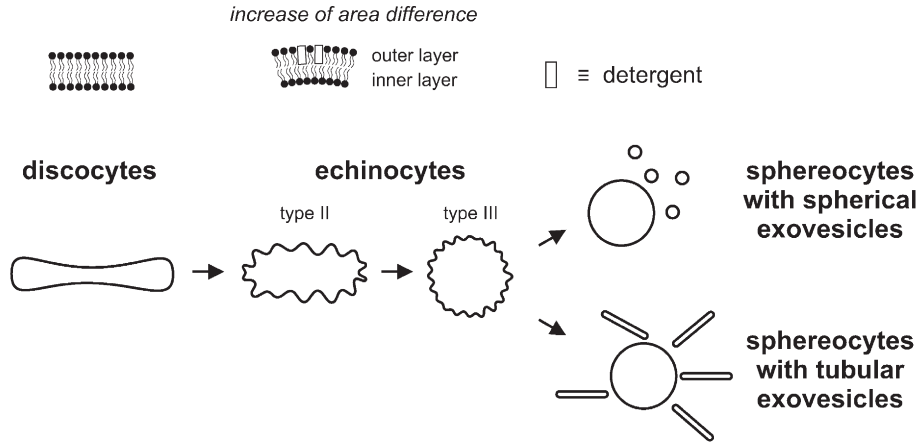


Fig. 1. Schematic figure of erythrocyte shape transformations due to preferential intercalation of a detergent into the outer membrane layer. At low detergent concentrations, echinocytes of type I and II (see [1]) appear in the erythrocyte suspension, while at higher molecular concentrations, echinocytes of type III are the most frequent. At still higher molecular concentrations, i.e. at sublytic molecular concentrations, the budding (exovesiculation) and release of spherical or tubular vesicles start (see also [15,19], and references therein). As a result, the erythrocytes are transformed into spherocytes.

where

$$H = \frac{1}{2}(C_1 + C_2), \quad (3)$$

is the local mean curvature of the membrane,  $C_1$  and  $C_2$  are the two principal curvatures describing the local shape of the membrane surface (Fig. 2),  $\langle H \rangle = \frac{1}{A} \int H dA$  is the average mean curvature,  $H_0$  is the effective spontaneous mean curvature [11],  $k_c$  is the membrane isotropic bending constant,  $k_n$  is the coefficient of nonlocal bending rigidity [6] and  $A$  is the membrane area.

For thin and not too strongly curved bilayers the average mean curvature  $\langle H \rangle$  is proportional to the difference between the two membrane monolayer areas ( $\Delta A$ ):

$$\langle H \rangle = \frac{\Delta A}{2A\delta}, \quad (4)$$

where  $\delta$  is the distance between the two monolayer neutral surfaces. The normalized average mean curvature  $\langle h \rangle = R_0 \langle H \rangle$  is equal to the normalized area difference  $\Delta a = \Delta A / 8\pi\delta R_0$ , where  $R_0$  is defined as:

$$R_0 = \sqrt{A/4\pi}. \quad (5)$$

The normalized effective spontaneous mean curvature  $h_0 = R_0 H_0$  is equal to the normalized optimal area difference  $\Delta a_0$ :

$$h_0 = \Delta a_0 = \Delta A_0 / 8\pi\delta R_0. \quad (6)$$

The optimal area difference  $\Delta A_0$  is determined by the difference in the number of molecules, differences in area per molecule and the difference in the intrinsic molecular shapes in the outer and the inner monolayer (see also [11,10,8], and references therein). The normalized optimal area difference  $\Delta a_0$  (or normalized spontaneous mean curvature  $h_0$ ) therefore depends on the excess number of detergent bound molecules in the outer

layer ( $N$ ), determined with respect to the number of detergent molecules in the inner layer of the membrane bilayer:

$$\Delta a_0 = \Delta a_{0,\text{ref}} + NS_a / 8\pi\delta R_0. \quad (7)$$

where  $S_a$  is the average area per detergent molecule and  $\Delta a_{0,\text{ref}}$  is the value of  $\Delta a_0$  before intercalation of the detergent starts. As may be seen from Eq. (7), the value of  $\Delta a_0$  linearly increases with the excess number of detergent molecules bound into the outer layer of the membrane bilayer.

Fig. 3 shows (for illustration) the calculated erythrocyte shapes determined by minimization of the membrane elastic energy (bending and shear) for two different values of the relative optimal area difference  $\Delta a_0$ . The echinocyte shape is also additionally modulated by stretching of the membrane skeleton [11,3] and by membrane-embedded proteins [16].

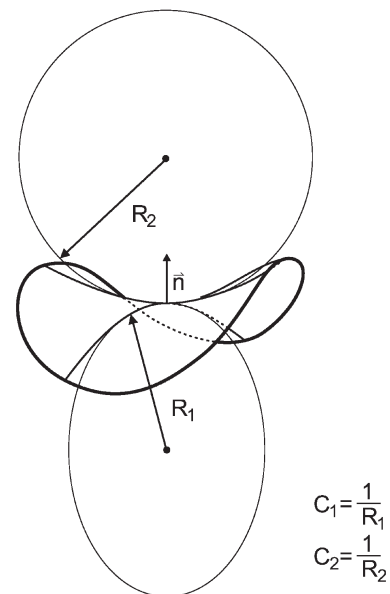


Fig. 2. Schematic illustration of the two principal curvatures of the membrane surface.

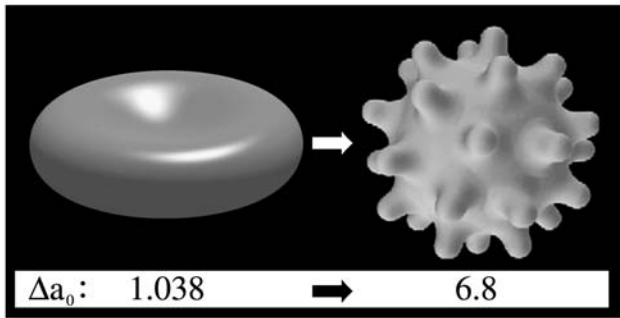


Fig. 3. The calculated erythrocyte shapes determined by minimization of the membrane elastic energy (bending and shear) for two different values of  $\Delta a_0$ : 1.038 and 6.8 and for  $k_t/k_c=8$  [12],  $\mu/k_c=10^{13} \text{ m}^{-2}$  [6] and a relative cell volume of 0.6. The cell shapes are calculated as described in Božič et al. [13] (for shape a) and Iglič et al. [15] (for shape b). The calculated equilibrium difference between the two cell membrane monolayer areas  $\Delta a$  are 1.038 (shape a) and 2.06 (shape b).

Fig. 4 shows the echinocyte shape transformation induced by adding dodecyl D-maltoside containing nanovesicles to the erythrocyte suspension. Nanovesicles were prepared separately at a sublytic concentration of dodecyl D-maltoside as described in detail elsewhere [17,18]. Apparently the progressive binding of dodecyl D-maltoside released from nanovesicles in the membranes of erythrocytes gradually increases the optimal area difference  $\Delta a_0$  of the erythrocyte membrane (see Eq. (7)) and consequently induces the observed discocyte–echinocyte shape transformation (see also Figs. 1 and 3).

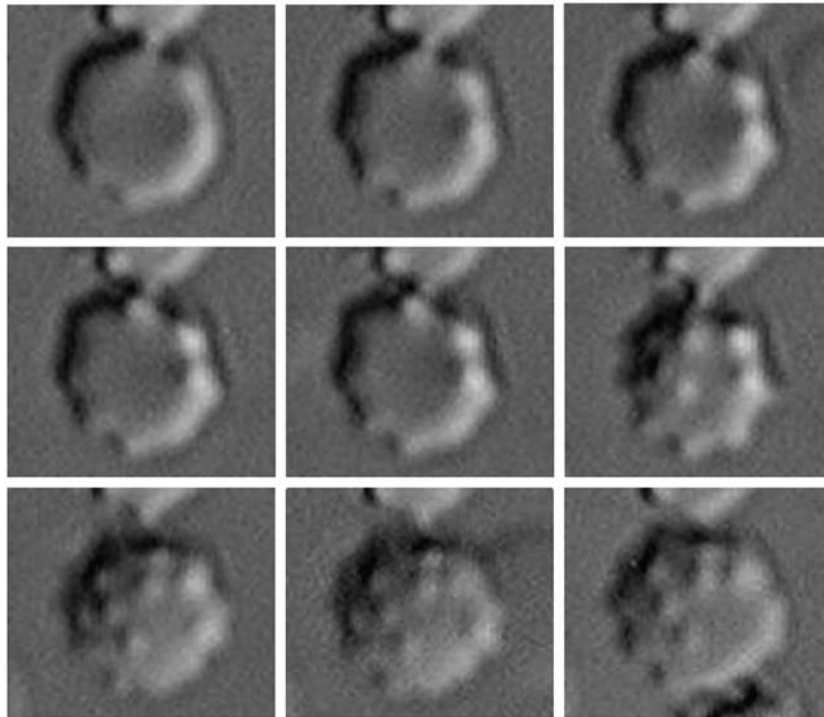


Fig. 4. Continuous discocyte–echinocyte shape transformation induced by incubation with dodecyl D-maltoside-containing nanovesicles. Erythrocytes were isolated from a healthy donor and isolated as described in Hägerstrand et al. [18]. Washed erythrocytes were diluted 200 times in buffer. A 5- $\mu\text{l}$  aliquot of the erythrocyte suspension was added to 45  $\mu\text{l}$  of 0.2 M glucose/0.2 M sucrose solution.

The spherical erythrocyte shape (spherocyte) at sublytic concentrations of echinocytogenic detergents arises due to reducing the size of echinocyte spicules. The spicules become smaller mainly due to release of daughter exovesicles from the cell surface (Fig. 1), predominantly from the echinocyte spicules (Fig. 5A). In the past, it was believed that progressive narrowing of echinocyte spicules due to release of the daughter exovesicles may lead to formation of thin tubular membrane spicules (protrusions) which are finally released from the cell surface as a whole in the form of long tubular exovesicles [14]. However, based on the results presented in Fig. 5, it can be concluded that tubular budding at the echinocyte spicules is the principal source of tubular exovesicles released from the membrane of erythrocytes.

Most of the hitherto studied echinocytogenic detergents induce spherical budding and nanoexovesicles, while strongly anisotropic detergent molecules (for example, dimeric detergents or detergents with a dimeric head group [21,19]) were found to induce mainly tubular buds and tubular nanoexovesicles (Fig. 5). The tubular budding observed does not need any additional driving (pulling) force.

Since the spherical and tubular daughter nanovesicles released from the erythrocyte membrane are highly depleted in the membrane skeleton [20,22], the shape of buds/vesicles is determined by the properties of the membrane bilayer. It is of interest to understand the mechanisms which determine the observed detergent-induced tubular budding of the bilayer membrane (Fig. 5). It is generally accepted [23–25,19] that the standard theory of isotropic membrane elasticity which [26] is

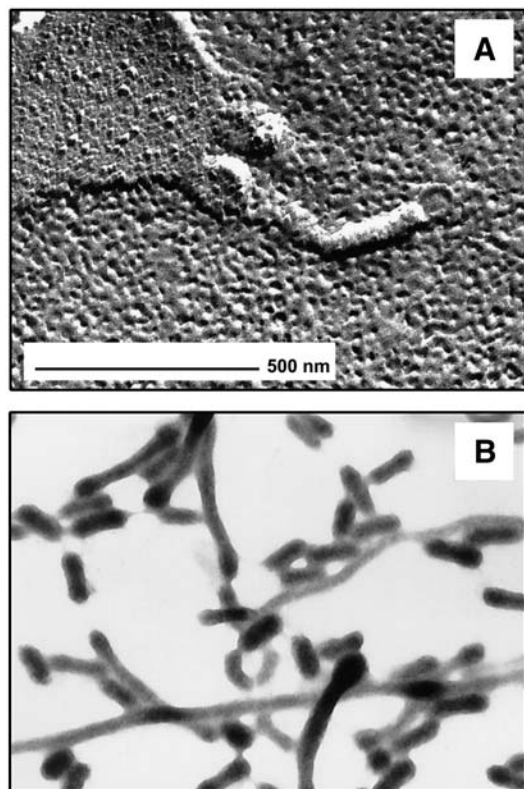


Fig. 5. TEM micrograph of freeze fracture replicas showing the tubular bud on top of an echinocyte spicule (A) (adapted from Kralj-Igljč et al. [19]) and a TEM micrograph of a dried sample showing free tubular nanoexovesicles released from the membrane (B). The radius of the tubular nanovesicles is about 40 nm. The budding/vesiculation was induced by adding 40  $\mu$ M dodecyl D-maltoside to an erythrocyte suspension. The molecule of dodecyl D-maltoside has a dimeric head group, therefore it is strongly anisotropic (see also panel A, Fig. 6).

based on a description of the membrane as a bilayer composed of two compressible isotropic monolayers does not provide an explanation for tubular budding (as observed in this work) if no pulling force is applied [23–25,19]. Therefore, in this work, we suggest a possible mechanism that may explain the observed detergent-induced tubular budding of the erythrocyte membrane with no pulling force required for the formation of these structures.

### Theoretical predictions

It was recently suggested that tubular budding may be theoretically explained by the accumulation of anisotropic membrane constituents in the tubular budding region [19]. Without the anisotropic membrane constituents, spherical budding is always energetically favourable [23,25,19].

Based on these suggestions, in this work we propose a possible mechanism that may explain the observed detergent-induced tubular budding of the erythrocyte membrane. The proposed mechanism is based on the energetically favourable self-assembly of anisotropic membrane nanodomains into larger domains forming nanotubular membrane protrusions. No pulling force is required in the model. Here, the nanodomain (sometimes also called raft element [18]) is defined as a very

small flexible membrane domain composed of different membrane components ([18,27,28,29], and references therein).

Much experimental and theoretical evidence indicates the existence of membrane micro- and nanodomains ([30,29,31–35,18], and references therein). Considering the biological membrane only as a mixture of different types of individual molecules with different intrinsic shapes and without explicitly taking into account the possibility of their self-assembly into mixed energetically favourable membrane micro- and/or nanodomains (which may be composed of many different types of molecules) would overestimate the role of the individual molecular intrinsic shape in the mechanics of biological membranes and neglect the role of direct interactions between the membrane constituents. For example, membrane lipids, which comprise an impressively large number of molecular species with different intrinsic shapes [36] (see also Fig. 6A), may self-assemble into various micro- and nanodomains with an average intrinsic shape (spontaneous curvature) of the domain which is different from the intrinsic shapes of the lipids constituting the domain (Fig. 7) [37]. A proper theoretical description of the mechanics of biological membranes should therefore also take into account the possibility that membrane molecules may form small (energetically favourable) micro- and nanodomains. However, because of the very large number of different types of molecules constituting the biological membrane [36], it would be an extremely hard task to consider in the theoretical model simultaneously the various intrinsic shapes of all the membrane molecules and also the different kinds of direct interactions between them (which may lead to energetically favourable formation of different membrane micro- and nanodomains). Consequently, in the theoretical approach applied in the present work, we introduce for the sake of simplicity the concept of a flexible membrane nanodomain which is defined as a complex of membrane molecules (lipids, proteins). Such flexible membrane nanodomains (see also Fig. 6B) are then considered as membrane building blocks.

In the model we assume that membrane nanodomains (Fig. 6B), as a result of their structure and local interactions energetically prefer a local geometry that is described by the two intrinsic principal curvatures ( $C_{1m}$  and  $C_{2m}$ ). The intrinsic principal curvatures (spontaneous curvatures) ( $C_{1m}$  and  $C_{2m}$ ) are in general different ( $C_{1m} \neq C_{2m}$ ) (Fig. 6). If they are identical ( $C_{1m} = C_{2m}$ ), the nanodomain is called isotropic. If  $C_{1m} \neq C_{2m}$ , the nanodomain is called anisotropic. The orientation of the anisotropic nanodomain is important for its energy. An anisotropic nanodomain (Fig. 6B) will, on the average, spend more time in the orientation that is energetically more favourable than in any other orientation.

The predominant binding of detergent molecules in the outer monolayer increases the optimal difference between the two membrane monolayer areas ( $\Delta A_0$ ) and thus makes the formation of tubular membrane protrusions (which corresponds to a high difference between the two cell membrane monolayer areas  $\Delta A$ ) energetically favourable. In addition it is also possible that the detergent molecules bound in the cell membrane may induce the formation of new nanodomains and/or increase the lateral mobility of already existing nanodomains. The increased lateral

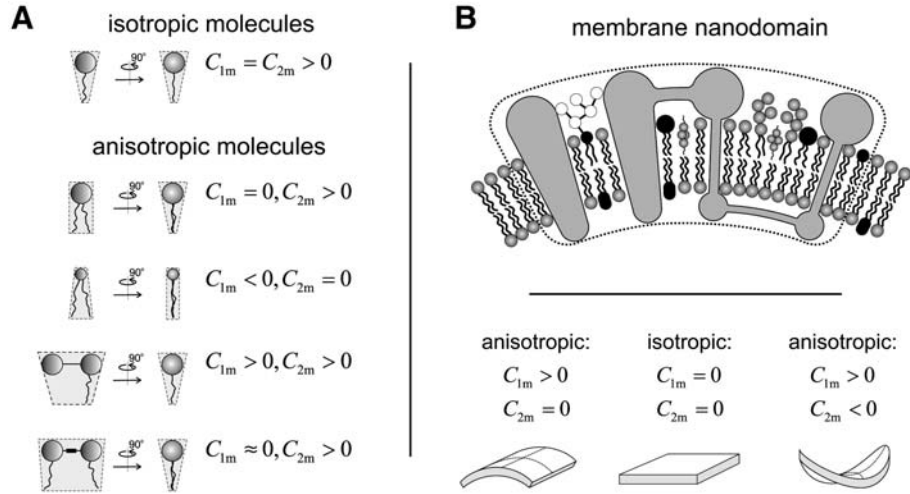


Fig. 6. Schematic representation of different intrinsic shapes of some detergent and phospholipid molecules (A) and of membrane-flexible nanodomains (B). Different intrinsic shapes are described by the two intrinsic principal curvatures  $C_{1m}$  and  $C_{2m}$ .

mobility of the nanodomains may be due to the detergent-induced changes in the skeleton–bilayer interactions, or due to the changed physical properties of the nanodomains influenced by the incorporated detergent molecules.

Based on experimental results which show that strongly anisotropic detergent molecules such as dimeric detergents or detergents with a dimeric head group (like dodecyl D-maltoside) [21,19] induce mainly tubular buds and tubular nanoexovesicles (Fig. 5), we assume that anisotropic detergents may induce in the erythrocyte membrane the formation of an anisotropic complex of molecules that forms a nanodomain (Fig. 6B).

**The energy of a single anisotropic nanodomain**

In this work the membrane nanodomain is considered as a small and thin flexible shell with the area  $a_0$  which can attain various equilibrium shapes that in general do not fit into flat or spherical shape (see also [38,41,39]) (Fig. 6B). Therefore its intrinsic shape could be described by the two intrinsic principal curvatures (spontaneous curvatures)  $C_{1m}$  and  $C_{2m}$  (Fig. 6B) and by the orientation of the nanodomain in the principal system of the actual local membrane curvature tensor  $\underline{C}$  (Fig. 7).

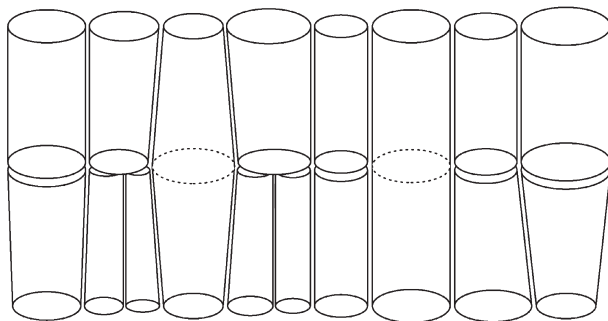


Fig. 7. The average intrinsic shape of the membrane domain may be different from the intrinsic shapes of the molecules (lipids and proteins) which constitute the domain (adapted from Kuypers et al. [37]).

Accordingly we define the elastic energy of a small plate-like membrane nanodomain (Fig. 6B) with area  $a_0$  as the energy of mismatch between the actual local curvature of the membrane (Fig. 2) and the intrinsic (spontaneous) curvature of the nanodomain which can be characterized by the tensor  $\underline{M} = \underline{R}\underline{C}_m\underline{R}^{-1} - \underline{C}$  where the tensor  $\underline{C}$  describes the actual curvature, the tensor  $\underline{C}_m$  describes the intrinsic curvature of the nanodomain (Fig. 6B), while

$$\underline{R} = \begin{bmatrix} \cos\omega & -\sin\omega \\ \sin\omega & \cos\omega \end{bmatrix}, \tag{8}$$

is the rotation matrix. The angle  $\omega$  describes the orientation of the single nanodomain with respect to the local principal axes of the membrane (Fig. 8). In the respective principal systems the matrices that represent curvature tensors  $\underline{C}$  and  $\underline{C}_m$  include only the diagonal elements (for tensor  $\underline{C}$  the elements  $C_1$  and  $C_2$  and for tensor  $\underline{C}_m$  the elements  $C_{1m}$  and  $C_{2m}$ ). The principal systems of these two tensors are in general rotated in

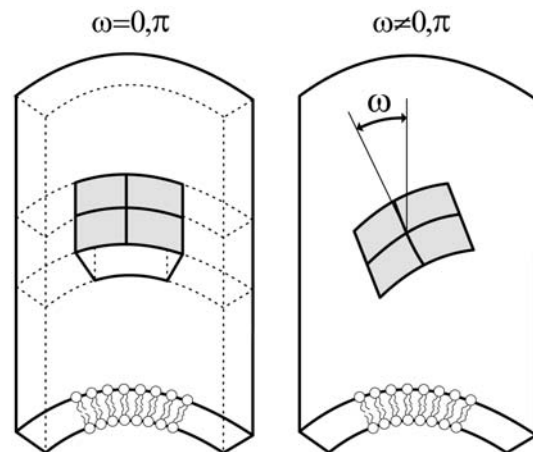


Fig. 8. Schematic figure of different orientations of an anisotropic nanodomain with intrinsic principal curvatures  $C_{1m} > 0$  and  $C_{2m} = 0$  in the curvature field of the membrane. The shape of the membrane is cylindrical ( $C_1 > 0$  and  $C_2 = 0$ ).

the tangent plane of the membrane surface by an angle  $\omega$  with respect to each other.

The elastic energy of the membrane nanodomain per unit area ( $w$ ) should be a scalar quantity. Therefore each term in the expansion of  $w$  must also be scalar [40], i.e. invariant with respect to all transformations of the local coordinate system. In this work, the elastic energy density  $w$  is approximated by an expansion in powers of all independent invariants of the tensor  $\underline{M}$  of the second order in the components of  $\underline{M}$ .

The trace and the determinant of the tensor are taken as the set of invariants [41]:

$$w = \mu_0 + \frac{K_1}{2} (\text{Tr}\underline{M})^2 + K_2 \text{Det}\underline{M}, \quad (9)$$

where  $\mu_0$  is the minimal possible value of  $w$ ,  $K_1$  and  $K_2$  are constants. For the sake of simplicity  $\mu_0=0$ . Taking into account the definition of the tensor  $\underline{M}$  it follows from Eq. (9) that the elastic energy of the single membrane (in general anisotropic) nanodomain can be written as:

$$E = \left[ (2K_1 + K_2)(H - H_m)^2 - K_2(D^2 - 2DD_m \cos 2\omega + D_m^2) \right] a_0, \quad (10)$$

where

$$D = \frac{1}{2}(C_1 - C_2), \quad (11)$$

is the membrane curvature deviator,  $H_m = (C_{1m} + C_{2m})/2$  is the intrinsic (spontaneous) mean curvature and  $D_m = (C_{1m} - C_{2m})/2$  is the intrinsic (spontaneous) curvature deviator and  $H = (C_1 + C_2)/2$ , as already defined above.

It can be seen from Eq. (10) that the material properties of an anisotropic flexible membrane nanodomain can be expressed in a simple way by only two intrinsic curvatures  $C_{1m}$  and  $C_{2m}$ . Fig. 6B shows schematically cylindrical, flat and saddle-like intrinsic (spontaneous) shapes of a flexible membrane nanodomain.

The optimal values of the membrane mean curvature  $H = (C_1 + C_2)/2$ , the curvature deviator  $D = (C_1 - C_2)/2$  and the nanodomain orientation angle  $\omega$  corresponding to the minimum of the function  $E$  for given values of  $H_m = (C_{1m} + C_{2m})/2$  and  $D_m = (C_{1m} - C_{2m})/2$  can be calculated from the necessary conditions for the extremum of the function  $E$  [42]:

$$\frac{\partial E}{\partial H} = 2a_0(2K_1 + K_2)(H - H_m) = 0, \quad (12)$$

$$\frac{\partial E}{\partial D} = -K_2 a_0 (2D - 2D_m \cos 2\omega) = 0, \quad (13)$$

$$\frac{\partial E}{\partial \omega} = -4a_0 K_2 D D_m \sin 2\omega = 0, \quad (14)$$

and the sufficient conditions for the minimum of  $E$  [43]:

$$\frac{\partial^2 E}{\partial H^2} = 2a_0(2K_1 + K_2) > 0, \quad (15)$$

$$\left( \frac{\partial^2 E}{\partial H^2} \right) \left( \frac{\partial^2 E}{\partial D^2} \right) - \left( \frac{\partial^2 E}{\partial H \partial D} \right)^2 = -4K_2 a_0^2 (2K_1 + K_2) > 0, \quad (16)$$

$$\begin{aligned} \frac{\partial^2 E}{\partial H^2} \left[ \left( \frac{\partial^2 E}{\partial D^2} \right) \left( \frac{\partial^2 E}{\partial \omega^2} \right) - \left( \frac{\partial^2 E}{\partial D \partial \omega} \right)^2 \right] \\ = 16K_2^2 a_0^2 \frac{\partial^2 E}{\partial H^2} (DD_m \cos 2\omega - D_m^2 \sin^2 2\omega) > 0, \end{aligned} \quad (17)$$

where

$$\frac{\partial^2 E}{\partial H \partial D} = 0, \quad \frac{\partial^2 E}{\partial H \partial \omega} = 0 \quad (18)$$

were taken into account. Considering only positive values of  $\omega$ , it follows from Eqs. (12)–(14) and (17) that the function  $E$  has minimal values for (see also Figs. 6 and 8):

$$H = H_m, \quad D = D_m, \quad \omega = 0, \pi, 2\pi, \quad (19)$$

where  $\omega=0$  and  $\omega=2\pi$  describe the same orientation and where [42]

$$K_1 > -K_2/2, \quad K_2 < 0. \quad (20)$$

If the flexible membrane nanodomain has  $C_{1m} > 0$  and  $C_{2m} > 0$  (see Fig. 6), the energetically favourable membrane shape would be a tubular membrane shape or a collapsed tubular membrane shape in the form of a twisted strip, where in the latter case the nanodomains would not be distributed at the edges of the strip (see also [39]).

The membrane nanodomain adapts its shape in order to fit its curvature to the actual membrane curvature (which is also influenced by the nanodomains). Since all orientations of nanodomain do not have the same energy (see Eq. (10) and Fig. 8), the partition function of a single nanodomain can be written in the form:

$$Q = \frac{1}{\omega_0} \int_0^{2\pi} \exp\left(-\frac{E(\omega)}{kT}\right) d\omega, \quad (21)$$

with  $\omega_0$  as an arbitrary angle quantum. The free energy of the membrane nanodomain is then obtained by the expression

$$f = -kT \ln Q. \quad (22)$$

Combining Eqs. (10), (21) and (22) allows us to write the free energy of the single flexible membrane nanodomain as (up to the constant terms):

$$\begin{aligned} f = (2K_1 + K_2)(H - H_m)^2 a_0 \\ - K_2(D^2 + D_m^2) a_0 - kT \ln \left( I_0 \left( \frac{2K_2 D D_m a_0}{kT} \right) \right). \end{aligned} \quad (23)$$

### Self-assembly of anisotropic nanodomains into tubular membrane protrusions

In the model we consider self-assembly of  $N$  membrane nanodomains into cylindrical membrane protrusions of equal radius  $r$ . The nanodomains are initially distributed in the (nearly) flat membrane. For the sake of simplicity it is taken that the nanodomain protrudes through both layers (see also Fig. 6B). We also assume that the nanodomains are laterally mobile over the membrane surface. For cylindrical protrusion,  $H=D$  everywhere on the membrane except on the tip and at the base of the protrusion, while in the flat regions  $H=D=0$  (Fig. 9).

For the sake of simplicity we assume  $K_1 \approx -K_2$ , therefore the energy of a single nanodomain (Eq. (23)) can be written in the form:

$$f = \frac{\xi}{2}(H - H_m)^2 + \frac{\xi}{2}(D^2 + D_m^2) - kT \ln \left( I_0 \left( \frac{\xi D_m D}{kT} \right) \right), \quad (24)$$

where  $\xi = 2a_0 K_2$  is the interaction constant.

Nanodomains in aggregates interact with neighbouring nanodomains. We denote the corresponding interaction energy per nanodomain (monomer) in the aggregate composed of  $i$  nanodomains as  $\chi(i)$  where we assume that the energy  $\chi(i)$  depends on the size of the aggregate  $i$ . Hence the mean energy per nanodomain in the cylindrical aggregate (where  $H=D$ ) composed of  $i$  nanodomains can be written as:

$$\mu_i = f_c - \chi(i), \quad (25)$$

where  $f_c = f(H=D)$  and  $\chi(i) > 0$ . We assume that in the planar regions of the membrane (having  $H=D=0$ ) the concentration of nanodomains is always below the critical aggregation concentration and therefore the nanodomain cannot form two-dimensional flat aggregates. The mean energy per nanodomain

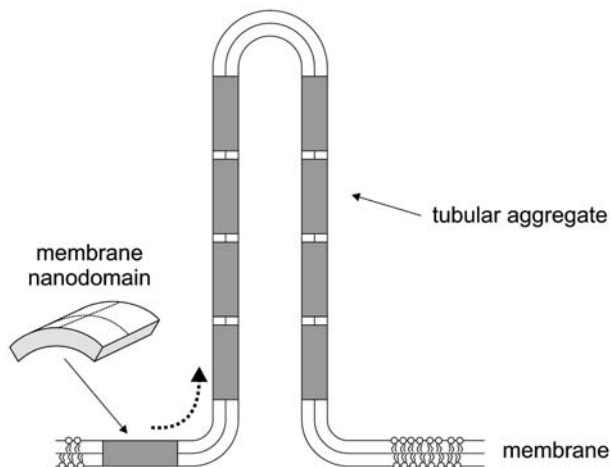


Fig. 9. Schematic figure of an energetically favourable self-assembly of anisotropic membrane nanodomains (characterized by  $C_{1m} > 0$  and  $C_{2m} = 0$ ) into larger membrane domain forming tubular aggregate.

in the flat membrane regions is therefore  $\tilde{\mu}_1 = f_p$ , where  $f_p = f(H=D=0)$ .

The concentration (mole fraction) of monomeric nanodomains in the flat membrane regions is

$$\tilde{x}_1 = \frac{\tilde{N}_1}{M}, \quad (26)$$

where  $\tilde{N}_1$  is the number of monomeric nanodomains in flat regions and  $M$  is the number of (lattice) sites in the whole system. The size distribution of cylindrical aggregate on the scale of concentration (mole fraction) is expressed as

$$x_i + \frac{iN_i}{M}, \quad (27)$$

where  $N_i$  denotes the number of cylindrical aggregates with aggregation number  $i$ , i.e. the number of tubular membrane protrusions ( $N_i$ ) consisting of  $i$  nanodomain each. The concentrations  $\tilde{x}_i$  and  $x_i$  should fulfil the conservation conditions for the total number of nanodomains in the membrane:

$$\tilde{x}_i + \sum_{i=1}^{\infty} x_i = N/M, \quad (28)$$

The free energy ( $F$ ) of all nanodomains in the membrane can thus be written as:

$$F = M[\tilde{x}_1 \tilde{\mu}_1 + kT \tilde{x}_1 (\ln \tilde{x}_1 - 1)] + M \sum_{i=1}^{\infty} \left[ x_i \mu_i + kT \frac{x_i}{i} (\ln \frac{x_i}{i} - 1) \right] - \mu M \left( \tilde{x}_1 + \sum_{i=1}^{\infty} x_i \right), \quad (29)$$

where  $\mu$  is the Lagrange parameter. Minimization of  $F$  with respect to  $\tilde{x}_1$  and  $x_i$ :

$$\frac{\partial F}{\partial \tilde{x}_1} = 0, \quad \frac{\partial F}{\partial x_i} = 0 \quad i = 1, 2, 3, \dots \quad (30)$$

leads to equilibrium distributions:

$$\tilde{x}_1 = \exp \left( -\frac{f_p - \mu}{kT} \right) \quad (31)$$

$$x_i = i \exp \left( -\frac{i}{kT} [f_c - \chi - \mu] \right) \quad (32)$$

where we assumed for simplicity that  $\chi(i)$  is a constant. The quantity  $\mu$  can be expressed from Eq. (31) and inserted in Eq. (32) to get:

$$x_i = i \left[ \tilde{x}_1 \exp \left( \frac{f_p + \chi - f_c}{kT} \right) \right]^i \quad (33)$$

Since  $x_i$  can never exceed unity it follows from Eq. (33) that when  $\tilde{x}_1$  approaches  $\exp[(f_c - f_p - \chi)/kT]$  it cannot be

increased further. The maximal possible value of the concentration of monomeric nanodomains in flat parts of the membrane  $\tilde{x}_1$  is therefore:

$$\tilde{x}_c \approx \exp\left(\frac{\Delta f - \chi}{kT}\right), \quad (34)$$

where  $\Delta f = f_c - f_p$  is the difference between the energy of the single nanodomain on the cylindrical protrusion and the energy of the nanodomain in the flat membrane region. The concentration  $\tilde{x}_c$  is the critical aggregation concentration [44]. In the case of cylindrical aggregates where  $H = D = 1/2r$  ( $r$  is the radius of the tubular membrane protrusion)

$$\Delta f = \zeta H(H - H_m) - kT \ln[I_0(\zeta D_m D / kT)]. \quad (35)$$

For  $1/2r > H_m$  the value of  $\Delta f$  is always negative. If  $\tilde{x}_1$  is above  $\tilde{x}_c$ , the formation of a very long cylindrical protrusion(s) composed of anisotropic membrane nanodomains is energetically favourable. It can be seen from Eq. (34) that longitudinal growth of the cylindrical membrane protrusion is promoted by the energy difference  $\Delta f$ , as well as by the strength of the direct interaction between the nanodomains  $\chi$ . The critical concentration  $\tilde{x}_c$  strongly decreases with increasing  $D_m$  (Fig. 10).

#### Discussion: Possible application of the proposed mechanism of stability of nanotubes in cellular systems

A physical mechanism similar to that as proposed to explain the growth and stability of the observed tubular membrane protrusions can also be responsible for the observed tendency for formation of a very long neck connecting a daughter vesicle and the mother membrane [47,31,48,49]. Elongation of the neck connecting two compartments could also play an important role in the formation and stabilization of the thin tubes that connect

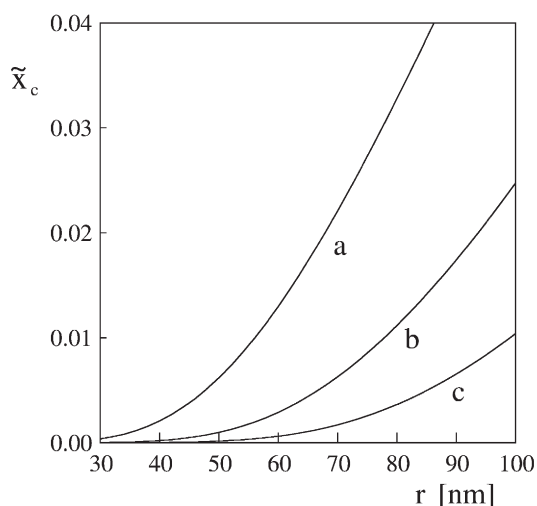


Fig. 10. Critical aggregation mole fraction (critical aggregation concentration) for self-assembly of anisotropic membrane nanodomains into larger membrane domains forming cylindrical aggregates calculated as a function of the radius of cylindrical aggregates ( $r$ ). The intrinsic shape of the single nanodomains are characterized by  $H_m = D_m$  of  $0.06 \text{ nm}^{-1}$  (a),  $0.08 \text{ nm}^{-1}$  (b) and  $0.1 \text{ nm}^{-1}$  (c). The values of other model parameters are:  $\xi = 5000kT \text{ nm}^2$  [45] and  $\chi = 1kT$  [46].

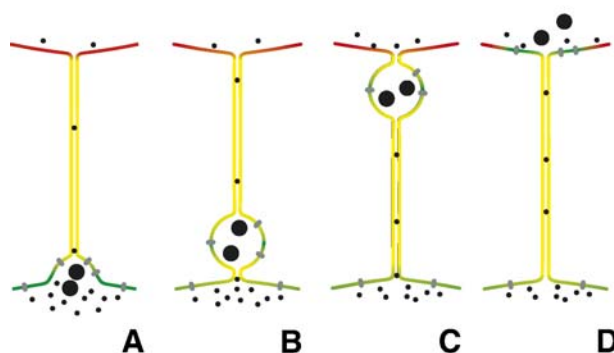
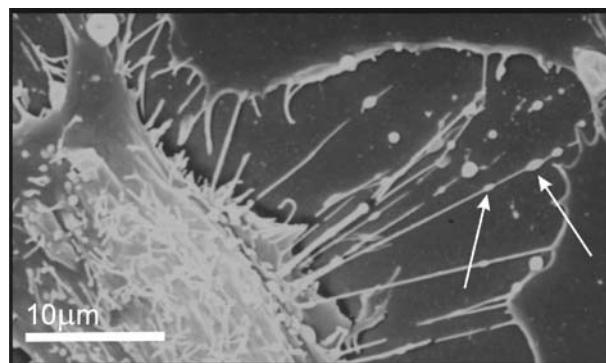


Fig. 11. Tubular structures with carrier vesicles (arrows) as observed in cultures of human urothelial line RT4 cells (upper, bar =  $10 \mu\text{m}$ ) and the corresponding schematic illustration of nanotube-directed transport of carrier vesicles (A–C) and direct transport through nanotubes (D).

cells or cell organelles (Fig. 11). Such tubes might be important in the transport of matter (Fig. 11) and information in cellular systems.

Namely, the results of some recent studies indicate that vesicular transport between cell organelles over longer distances is not random and that it takes place between specific surface regions of the cell organelles [50,45]. Such organized transport may be achieved by nanotube-directed transport of carrier vesicles (gondolas) (Figs. 11A–C) (see also [51]) or by direct transport through nanotubes (Fig. 11D) (see also [51,52,53]).

The initiation of gondola formation (Fig. 11A) may be based on similar physical mechanisms as those governing the formation of free membrane daughter vesicles, which are created in the processes of budding. In contrast to the latter process, however, in gondolas the connection to the parent membrane from which they originate is not disrupted when the vesicle is detached from the parent membrane (Fig. 11B). The creation of gondolas, corresponding to transient excited states, may also be induced by a sudden tension in the membrane tubes [54,55]. Such excited states of the membrane are relaxed after a certain time; slight undulations are relaxed in seconds while sphere-like blobs are relaxed in minutes [54].

Once the gondola is formed, its movement along the nanotube (Fig. 11B) requires no additional bending energy. Nevertheless, some process is needed to provide the energy (required to overcome frictional forces) for the gondola to travel along the nanotube. It is possible that the gondola movement is driven by the difference in chemical potential between the

molecules packed inside the gondola and the molecules in the interior of the target cell, or the difference in chemical potential between the molecules composing the membrane of the gondola and the molecules in the membrane of the target cell.

The final event is the fusion of the gondola with the target membrane. In this process, those molecules of the gondola's membrane which originate from the parent, nearly flat membrane, distribute again in an almost flat (target) membrane (Fig. 11C). This may be energetically favourable and constitutes a part of the driving mechanism which facilitates the fusion of the gondola with the target membrane. Prior to the fusion of the gondola with the target cell membrane, no neck formation is needed when a gondola is attached to the target membrane, contrary to the case of a free transport vesicle, since in the former case the neck is already formed, i.e. the neck is a part of the nanotube connecting the gondola to the membrane of the target cell. It can therefore be concluded that the transport of material in gondolas (or the transport of molecules composing the membrane of gondolas) may be energetically advantageous over free vesicle transport.

## Conclusion

In this work we suggest a possible mechanism that may explain the observed detergent-induced tubular budding of the erythrocyte membrane. The proposed mechanism is based on the energetically favourable self-assembly of anisotropic membrane nanodomains into larger membrane domains forming nanotubular membrane protrusions.

The described mechanism of growth and stability of tubular membrane protrusions may also be relevant for formation and stabilization of thin tubes that connect cells or cell organelles and might be important in intracellular and intercellular transport and communication. Since the nanotubes are difficult to visualize and are also very fragile, the proposed mechanism of directed vesicle transport may in the past have been overlooked in biological systems, but it could be expected that in the future it will receive more attention due to its vital importance.

## Acknowledgments

This work was supported by ARRS grants P2-0232-1538 and BI-US/05-06/014. This paper is based on a presentation at the Red Cell Conference held at the Yale University in New Haven Connecticut November 3–4, 2006.

## References

- [1] M. Bessis, *Living Blood Cells and Their Ultrastructure*, Springer, New York, 1973.
- [2] A. Iglič, A possible mechanism determining the stability of spiculated red blood cells, *J. Biomech.* 30 (1997) 35–40.
- [3] N. Mohandas, E.A. Evans, Mechanical properties of the red cell membrane in relation to molecular structure and genetic defects, *Ann. Rev. Biophys. Biomed. Struct.* 23 (1994) 787–818.
- [4] D.E.N. Discher, N. Mohandas, E.A. Evans, Molecular maps of red cell deformability: hidden elasticity and in situ connectivity, *Science* 266 (1994) 1032–1035.
- [5] D.E.N. Discher, N. Mohandas, Kinematics of red cell aspiration by fluorescence-imaged microdeformation, *Biophys. J.* 71 (1996) 1680–1694.
- [6] E.A. Evans, R. Skalak, *Mechanics and Thermodynamics of Biomembranes*, CRC Press, Boca Raton, 1980.
- [7] R.E. Waugh, Elastic energy of curvature-driven bump formation on red blood cell membrane, *Biophys. J.* 70 (1996) 1027–1035.
- [8] W. Helfrich, Blocked lipid exchange in bilayers and its possible influence on the shape of vesicles, *Z. Naturforsch.* 29c (1974) 510–515.
- [9] B.T. Stokke, A. Mikkelsen, A. Elgsaeter, The human erythrocyte membrane skeleton may be an ionic gel, *Eur. Biophys. J.* 13 (1986) 203–218.
- [10] L. Miao, U. Seifert, M. Wortis, H.G. Döbereiner, Budding transitions of fluid–bilayer vesicles: effect of area difference elasticity, *Phys. Rev., E* 49 (1994) 5389–5407.
- [11] R. Mukhopadhyay, G. Lim, M. Wortis, Echinocyte shapes: bending, stretching and shear determine spicule shape and spacing, *Biophys. J.* 82 (2002) 1756–1772.
- [12] W.C. Hwang, R.E. Waugh, Energy of dissociation of lipid bilayer from the membrane skeleton of red cells, *Biophys. J.* 72 (1997) 2669–2678.
- [13] B. Božič, V. Kralj-Iglič, S. Svetina, Coupling between vesicle shape and lateral distribution of mobile membrane inclusions, *Phys. Rev., E* 73 (2006) 041915/1–11.
- [14] G.M. Wagner, D.T.Y. Chiu, M.C. Yee, B.H. Lubin, Red cell vesiculation – a common membrane physiological event, *J. Lab. Clin. Med.* 108 (1986) 315–324.
- [15] A. Iglič, V. Kralj-Iglič, H. Hägerstrand, Amphiphile induced echinocyte–spherocochinocyte transformation of red blood cell shape, *Eur. Biophys. J.* 27 (1998) 335–339.
- [16] H. Hägerstrand, M. Danieluk, M. Bobrowska-Hägerstrand, A. Iglič, A. Wróbel, B. Isomaa, M. Nikinmaa, Influence of band 3 protein absence and skeletal structures on amphiphile and  $Ca^{2+}$  induced shape alteration in erythrocytes: a study with lamprey (*Lampetra fluviatilis*), trout (*Onchorhynchus mykiss*) and human erythrocytes, *Biochim. Biophys. Acta* 1466 (2000) 125–138.
- [17] H. Hägerstrand, B. Isomaa, Vesiculation induced by amphiphiles in erythrocytes, *Biochim. Biophys. Acta* 982 (1989) 179–186.
- [18] H. Hägerstrand, L. Mrowczynska, U. Salzer, R. Prohaska, K.A. Michelsen, V. Kralj-Iglič, A. Iglič, Curvature dependent lateral distribution of raft markers in the human erythrocyte membrane, *Mol. Membr. Biol.* 23 (2006) 277–288.
- [19] V. Kralj-Iglič, H. Hägerstrand, P. Veranič, K. Jezernik, D.R. Gauger, A. Iglič, Amphiphile-induced tubular budding of the bilayer membrane, *Eur. Biophys. J.* 34 (2005) 1066–1070.
- [20] H. Hägerstrand, V. Kralj-Iglič, M. Bobrowska-Hägerstrand, A. Iglič, Membrane skeleton detachment in spherical and cylindrical microexovesicles, *Bull. Math. Biol.* 61 (1999) 1019–1030.
- [21] V. Kralj-Iglič, A. Iglič, H. Hägerstrand, P. Peterlin, Stable tubular microexovesicles of the erythrocyte membrane induced by dimeric amphiphiles, *Phys. Rev., E* 61 (2000) 4230–4234.
- [22] D.W.L. Knowles, N. Tilley, N. Mohandas, J.A. Chasis, Erythrocyte membrane vesiculation: model for the molecular mechanism of protein sorting, *Proc. Natl. Acad. Sci. U. S. A.* 94 (1997) 12969–12974.
- [23] L. Miao, B. Fourcade, M. Rao, M. Wortis, R.K.P. Zia, Equilibrium budding and vesiculation in the curvature model of fluid lipid vesicles, *Phys. Rev., E* 43 (1991) 6843–6856.
- [24] I. Derényi, F. Jülicher, J. Prost, Formation and interaction of membrane tubes, *Phys. Rev. Lett.* 88 (2002) 238101/1–4.
- [25] I. Tsafir, Y. Caspi, M.A. Guedeau, T. Arzi, J. Stavans, Budding and tubulation of highly oblate vesicles by anchored amphiphilic molecules, *Phys. Rev. Lett.* 91 (2003) 138102/1–4.
- [26] E. Sackmann, Membrane bending energy concept of vesicle and cell shapes and shape transitions, *FEBS Lett.* 346 (1994) 3–16.
- [27] D.A. Brown, E. London, Structure and origin of ordered lipid domains in biological membranes, *J. Membr. Biol.* 164 (1998) 103–114.
- [28] K. Jacobson, C. Dietrich, Looking at lipid raft? *Trends Cell Biol.* 9 (1999) 87–91.
- [29] D. Corbeil, K. Röper, C.A. Fargeas, A. Joester, H.B. Huttner, Prominin: a

- story of cholesterol, plasma membrane protrusions and human pathology, *Traffic* 2 (2001) 82–91.
- [30] T. Harder, K. Simons, Caveolae, DIGs, and the dynamics of sphingolipid–cholesterol microdomains, *Curr. Opin. Cell Biol.* 9 (1997) 534–542.
- [31] W.B. Huttner, J. Zimmerberg, Implications of lipid microdomains for membrane curvature, budding and fission, *Curr. Opin. Cell Biol.* 13 (2001) 478–484.
- [32] B.U. Samuel, N. Mohandas, T. Harrison, H. McManus, W. Rosse, M. Reid, K. Haldar, The role of cholesterol and glycosylphosphatidylinositol-anchored proteins of erythrocyte rafts in regulating raft protein content and malarial infection, *J. Biol. Chem.* 276 (2001) 29319–29329.
- [33] U. Salzer, R. Prohaska, Segregation of lipid raft proteins during calcium-induced vesiculation of erythrocytes, *Blood* 101 (2003) 3751–3753.
- [34] U. Salzer, P. Hinterdorfer, U. Hunger, C. Borken, R. Prohaska, Ca<sup>++</sup>-dependent vesicle release from erythrocytes involves stomatin-specific lipid rafts, synexin (annexin VII), and sorcin, *Blood* 99 (2002) 2569–2577.
- [35] P. Sens, M.S. Turner, Theoretical model for the formation of caveolae and similar membrane invaginations, *Biophys. J.* 86 (2004) 2049–2057.
- [36] B. Roelofsens, F.A. Kuypers, J.A.F. Op den Kamp, L.L.M. Deenen, Influence of phosphatidylcholine molecular species composition on stability of the erythrocyte membrane, *Biochem. Soc. Trans.* 17 (1989) 284–286.
- [37] F.A. Kuypers, B. Roelofsens, W. Berendsen, J.A.F. Op den Kamp, L.L.M. van Deenen, Shape changes in human erythrocytes induced by replacement of the native phosphatidylcholine with species containing various fatty acids, *J. Cell Biol.* 99 (1984) 2260–2267.
- [38] W. Helfrich, J. Prost, Intrinsic bending force in anisotropic membranes made of chiral molecules, *Phys. Rev., A* 38 (1988) 3065–3068.
- [39] A. Iglič, M. Tzaphlidou, M. Remškar, B. Babnik, M. Daniel, V. Kralj-Iglič, Stable shapes of thin anisotropic nano-strips, *Fuller Nanotub. Carbon Nanostructures* 13 (2005) 183–192.
- [40] L.D. Landau, E.M. Lifshitz, *Theory of Elasticity*, 3rd ed. Butterworth-Heinemann, Oxford, 1997.
- [41] A. Iglič, B. Babnik, U. Gimsa, V. Kralj-Iglič, On the role of membrane anisotropy in the beading transition of undulated tubular membrane structures, *J. Phys. A, Math. Gen.* 38 (2006) 8527–8536.
- [42] A. Iglič, T. Slivnik, V. Kralj-Iglič, Elastic properties of biological membranes influenced by attached proteins, *J. Biomech.* (2007), doi:10.1016/j.jbiomech.2006.11.005.
- [43] D.V. Widder, *Advanced Calculus*, Prentice-Hall Inc, New York, 1947.
- [44] J.N. Israelachvili, *Intermolecular and Surface Forces*, Academic Press, London, 1997.
- [45] A. Iglič, M. Fošnarič, H. Hägerstrand, V. Kralj-Iglič, Coupling between vesicle shape and the non-homogeneous lateral distribution of membrane constituents in Golgi bodies, *FEBS Lett.* 574/1–3 (2004) 9–12.
- [46] K. Bohinc, V. Kralj-Iglič, S. May, Interaction between two cylindrical inclusions in a symmetric lipid bilayer, *J. Chem. Phys.* 119 (2003) 7435–7444.
- [47] H. Gad, P. Löw, E. Zotova, L. Brodin, O. Shupliakov, Dissociation between Ca<sup>2+</sup>-triggered synaptic vesicle exocytosis and clathrin-mediated endocytosis at a central synapse, *Neuron* 21 (1998) 607–616.
- [48] V. Kralj-Iglič, A. Iglič, M. Bobrowska-Hägerstrand, H. Hägerstrand, Tethers connecting daughter vesicles and parent red blood cell may be formed due to ordering of anisotropic membrane constituents, *Colloids Surf., A* 179 (2001) 57–64.
- [49] L. Rajendran, M. Masilamani, S. Solomon, R. Tikkanen, C.A. Stuermer, H. Plattner, H. Illges, Asymmetric localization of flotillins/reggies in preassembled platforms confers inherent polarity to hematopoietic cells, *Proc. Natl. Acad. Sci. U. S. A.* 100 (2003) 8241–8246.
- [50] H. Sprong, P. van der Sluijs, G. Meer, How proteins move lipids and lipids move proteins, *Nat. Cell Biol.* 2 (2001) 504–513.
- [51] A. Iglič, H. Hägerstrand, M. Bobrowska-Hägerstrand, V. Arrigler, V. Kralj-Iglič, Possible role of phospholipid nanotubes in directed transport of membrane vesicles, *Phys. Lett., A* 310 (2003) 493–497.
- [52] A. Rustom, R. Saffrich, I. Marković, P. Walther, H.H. Gerdes, Nanotubular highways for intracellular organelle transport, *Science* 303 (2004) 1007–1010.
- [53] M. Sun, J.S. Graham, B. Hegedüs, F. Marga, Y. Zhang, G. Forgacs, Multiple membrane tethers probed by atomic force microscopy, *Biophys. J.* 89 (2005) 4320–4329.
- [54] R. Bar-Ziv, E. Moses, Instability and pearling states produced in tubular membranes by competition of curvature and tension, *Phys. Rev. Lett.* 73 (1994) 1392–1395.
- [55] E. Evans, W. Rawicz, Entropy-driven tension and bending elasticity in condensed-fluid membranes, *Phys. Rev. Lett.* 64 (1990) 2094–2097.